A New Heuristic Approach for Low-Thrust Spacecraft Trajectory Optimization [1]

Peter Coppens * **Ben Hermans** ** **Jeroen Vandersteen** ***
Goele Pipeleers ** **Panagiotis Patrinos** *

* *STADIUS Center for Dynamical Systems, Signal Processing and Data Analytics, Department of Electrical Engineering (ESAT), KU Leuven, Leuven, Belgium.*
(e-mail: peter.coppens@kuleuven.be)
** *MECO Research Team, Department of Mechanical Engineering, KU Leuven, Leuven, Belgium and Flanders Make – DMMS-M, Leuven, Belgium.*
*** *ESTEC, European Space Agency, Noordwijk, Netherlands.*

Abstract: Electrical propulsion is gaining popularity in the satellite industry. Their high efficiency however comes at the cost of decreased thrust and longer transfer times. As such the interest in solving the large optimization problems associated with these long transfers has re-surged. This paper presents a heuristic approach to solving such low-thrust satellite trajectory optimization problems, based on control law blending and averaging. We derive the nonlinear program resulting from this approach and introduce PANOC, a recent optimization algorithm well suited for optimal control problems. The resulting controller is considerably faster than more classical, non-heuristic approaches, without a significant loss in optimality.

Keywords: real-time optimal control, numerical methods for optimal control, aerospace, optimal control theory, nonlinear predictive control.

1. INTRODUCTION

The competitive nature of the satellite industry has recently driven the development of electric propulsion (EP) technology (Feuerborn et al., 2013; Lev et al., 2017). These engines provide an efficient alternative to classical chemical propulsion at the cost of lower thrust and longer transfer times (Bruno, 2014). Finding the spirallike trajectories that are required to perform transfers using the new thrusters push current optimal control algorithms to their limit. Onboard trajectory calculation is especially challenging, since repeated solutions are required and hardware performance/memory is limited.

The challenging nature of these problems has already driven the development of many new optimal control methods to deal with large amounts of variables and long integration times. One method that is especially common is the collocated approach, where the trajectory is parametrized using polynomials, which should then satisfy the dynamics exactly at a number of nodes, resulting in many nonlinear constraints. This technique has been applied succesfully to many transfer scenarios (Conway, 2010; Betts and Erb, 2003; Schäff, 2016). Besides the collocated approach, many other approaches have been applied to satellite trajectory optimization as well. Results from the theory of variations, like Pontryagin's Maximum Principle (Chachuat, 2007), have been used to achieve both numerical (Mazzini, 2014; Huang et al., 2009) and analytical solutions (Edelbaum, 1965; Fernandes and Carvalho, 2018) for a couple of transfer scenarios. Another category of methods is the class of heuristic approaches. These parametrize the input based on certain control laws, which simplifies the associated optimization problems. Many variations of these techniques exist, like shape-based approaches (Vicens, 2016; Petropoulos and Longuski, 2004), where the control law is selected to enable an analytic evaluation of the states (sacrificing optimality in the process). Approaches based on Lyapunov feedback control have also been examined in the past (Petropoulos, 2005). Another approach employs control laws that are periodic in the true anomaly, which are combined with averaging methods to integrate the dynamics (Kluever and Conway, 2010; Kluever, 1998). The approach presented here lies in this category.

This paper presents a heuristic, sequential approach to deal with orbit raising problems. The approach is based on the work presented in (Kluever and Conway, 2010) which present numerical schemes applied to averaged orbital dynamics and (Pollard, 2000) who developed control laws applicable to orbit raising problems. The resulting algo-

[1] Peter Coppens' and Panagiotis Patrinos' research is supported by the Fonds Wetenschappelijk Onderzoek PhD grant 11E5520N and research projects G0A0920N, G086518N and G086318N; Research Council KU Leuven C1 project No. C14/18/068; Fonds de la Recherche Scientifique – FNRS and the Fonds Wetenschappelijk Onderzoek – Vlaanderen under EOS project no 30468160 (SeLMA). Ben Hermans' and Goele Pipeleers' research benefits from KU Leuven-BOF No. PFV/10/002, from project No. G0C4515N of the Research Foundation - Flanders (FWO - Flanders), from Flanders Make ICON: Avoidance of collisions and obstacles in narrow lanes, and from the KU Leuven Research project No. C14/15/067.

rithm borrows flexibility from direct approaches like the collocated approach and combines it with the efficiency of heuristic approaches, without a significant loss in optimality. We solve the optimization problems with a structured optimization algorithm called PANOC (Proximal Averaged Newton-type Method for Optimal Control) (Stella et al., 2017), which unlike other state-of-the-art solvers does not solve large systems of linear equations, reducing memory requirements. The terminal state constraints are enforced using the augmented Lagrangian method (ALM) (Bertsekas, 1996).

The paper is structured as follows: Section 2 presents the problem statement and derives the components required for the heuristic approach. Section 3 then presents the structured optimization algorithm as well as the method used to enforce the terminal state constraint. Section 4 validates the approach by applying it to a realistic transfer scenario and comparing the heuristic approach to the sequential approach applied directly to the unregularized dynamics. The capabilities of the approach in a closed-loop scheme are also illustrated. Section 5 draws some concluding remarks.

2. PROBLEM STATEMENT AND METHODOLOGY

This section formulates the transfer problem and introduces the Modified Equinoctial Elements (MEE), which we regularize using the Sundman transform. Then the control laws, developed by (Pollard, 2000), are derived for MEE and the averaging method is presented. Finally the sequential approach is derived such that it is compatible with the optimization algorithm presented in Section 3.

2.1 Orbital Dynamics

The motion of a satellite around the earth is approximately described by the two-body problem (Battin, 1999). It is well known that the resulting orbits are all conical sections and their evolution under a disturbance can be described using orbital elements. A survey of such elements is given in (Hintz, 2008), which concludes that the MEE, first presented in (Walker et al., 1985), are well suited for low-thrust trajectory optimization. They are defined in function of the classical orbital elements which consist of the Euler angles (Ω, i, ω) describing the orbital plane and (a, e, θ) describing the orbit and the position in that plane. Ω is called the argument of the ascending node, i is the inclination and ω is the argument of periapsis. The shape of the orbit is assumed to be an ellipse with eccentricity e and semi-major axis length a. The true anomaly θ then describes the position of the satellite on the orbit as the angle between the periapsis and the current position. The MEE are then defined as follows:

$$p = a(1-e^2), \quad f = e\cos(\omega+\Omega), \quad g = e\sin(\omega+\Omega),$$
$$h = \tan\frac{i}{2}\cos(\Omega), \quad k = \tan\frac{i}{2}\cos(\Omega), \quad L = \Omega+\omega+\theta,$$

The MEE variational equations are given in Gaussian form below (Betts and Erb, 2003):

$$\dot{p} = 2\tfrac{p\tau_t}{w}\sqrt{\tfrac{p}{\Gamma}}, \tag{1a}$$
$$\dot{f} = \sqrt{\tfrac{p}{\Gamma}}\left(\tau_r\sin L + ((w+1)\cos L + f)\tfrac{\tau_t}{w} - gv\right), \tag{1b}$$
$$\dot{g} = \sqrt{\tfrac{p}{\Gamma}}\left(-\tau_r\cos L + ((w+1)\sin L + g)\tfrac{\tau_t}{w} + fv\right), \tag{1c}$$
$$\dot{h} = \sqrt{\tfrac{p}{\Gamma}}\left(\tfrac{1+h^2+k^2}{2w}\right)\cos(L)\tau_n, \tag{1d}$$
$$\dot{k} = \sqrt{\tfrac{p}{\Gamma}}\left(\tfrac{1+h^2+k^2}{2w}\right)\sin(L)\tau_n, \tag{1e}$$
$$\dot{L} = \sqrt{\Gamma p}\left(\tfrac{w}{p}\right)^2 + \sqrt{p}\Gamma v, \tag{1f}$$

with $w = 1+f\cos L+g\sin L$, $v = \frac{\tau_n}{w}(h\sin L - k\cos L)$ and Γ the gravitational parameter of earth. The dependency of the states on time is omitted to simplify the notation. Note that the only singularities present in the MEE occur when $i = \pi$, *i.e. when the orbit flips direction.* Since this will not occur for most transfers it is not considered to be an issue. $\tau = (\tau_r, \tau_t, \tau_n) \in \mathbb{R}^{n_\tau}$ denotes the disturbing acceleration given in the Gaussian, or radial, tangential and normal (RTN) satellite-based coordinate system. The origin is therefore located at the satellite with the radial vector pointing away from the central body, the normal vector pointing in the direction of the moment of impulse vector and the tangential vector completing the right-handed system (Macdonald, 2014). For simplicity we will assume that the mass of the satellite remains constant. As such the length of the acceleration vector τ varies between 0 and τ_m, with τ_m the thrust-to-weight ratio of the satellite. This assumption does not affect the outcome of the optimization problem by much and the presented framework supports the inclusion of a changing mass.

The MEE dynamics can be regularized using the well known Sundman transform described in (Vicens, 2016). It is applied by multiplying the right side of the variational equations with:

$$\frac{dE}{dt} = \sqrt{\frac{\Gamma}{p(1-f^2-g^2)}}\frac{w}{p}, \tag{2}$$

which intuitively corresponds to integrating over the eccentric anomaly E of the elliptic orbit instead of time.

2.2 Control Laws

In (Pollard, 2000) four laws to describe the acceleration direction in the orbital plane are considered: tangential acceleration, acceleration in the direction of the velocity, acceleration in the direction of the semi-minor axis and acceleration in the direction of the semi-major axis. For MEE these laws are written as:

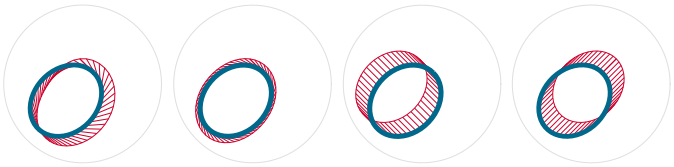
$$\begin{aligned} c_1 &= (0,1), \\ c_2 &= \frac{(f\sin L + g\cos L, f\cos L + g\sin L + 1)}{\sqrt{1+f^2+g^2+2g\sin L+2f\cos L}} \\ c_3 &= (\sin(L-\bar{\omega}), \cos(L-\bar{\omega})) \\ c_4 &= (\cos(L-\bar{\omega}), \sin(L-\bar{\omega})), \end{aligned} \tag{3}$$

where $\bar{\omega} = \tan^{-1}(g/f)$ [2]. To introduce the parameters, thereby increasing the degrees of freedom for the optimizer, blending is used. The idea is to consider:

$$Q_{rt}(x,p) = \frac{p_1c_1 + p_2c_2 + p_3c_3 + p_4c_4}{\max(\|p_1c_1 + p_2c_2 + p_3c_3 + p_4c_4\|, 10^{-10})}, \tag{4}$$

with $Q_{rt}(\cdot,\cdot)$ the in-plane control law and x the vector of orbital elements (p, f, g, k, h, L). The optimization

[2] To deal with the singularities associated with $\bar{\omega}$ we will later add it as an additional variable in the optimization algorithm.



(a) (b) (c) (d)

Fig. 1. Control laws by Pollard. The bold ellipse depicts the current orbit and the lines depict the acceleration vectors. From left to right the control laws are in the direction of the tangential, velocity, semi-minor and semi-major.

problem then becomes finding the optimal parameters $p_1(t), p_2(t), p_3(t), p_4(t)$. The max operator is there to avoid singularities. The acceleration directions for the four control laws defined in (3) are depicted in Figure 1. Pollard (2000) originally selected these laws to derive analytic expressions for the variational dynamics of the classical orbit elements. Their good variation in acceleration directions makes them suitable for our application since they provide enough degrees of freedom and approximate the optimal behaviour well.

The next step is the parametrization of the acceleration vector length. For this we consider bang-bang control, where the acceleration magnitude either takes its maximal value τ_m or 0. This behaviour is known to be optimal for many transfers and its optimality can be verified using calculus of variations as done in (Prussing, 2010), which suggests why the parametrization also performs well in practice. The acceleration control law developed in (Pollard, 2000) is given as:

$$Q_\tau(x(t), p(t)) = \begin{cases} \tau_m & -p_{E_0} \leq E \leq p_{E_0} \\ \tau_m & -p_{E_\pi} \leq \pi + E \leq p_{E_\pi} \\ 0 & \text{else} \end{cases}, \tag{5}$$

where E is the eccentric anomaly defined as:

$$E = 2\tan^{-1}\left(\sqrt{\frac{1+\sqrt{f^2+g^2}}{1-\sqrt{f^2+g^2}}} + \tan\left(\frac{L-\bar{\omega}}{2}\right)\right). \tag{6}$$

$p_{E_0}(t) \geq 0$ and $p_{E_\pi}(t) \geq 0$ are later added as variables in the optimization problem, with the additional constraint $p_{E_0} + p_{E_\pi} \leq \pi$. To deal with inclination changes, two more parameters $p_{rt}(t)$ and $p_n(t)$ that satisfy $p_{rt}^2 + p_n^2 = 1$ are added. The full control law then becomes:

$$\tau = Q_\tau(x,p)\left(Q_{rt}(x,p)p_{rt},\ p_n\right). \tag{7}$$

Note that Q_{rt} is a column vector of two elements and that $(Q_{rt}(x,p)p_{rt},\ p_n)$ denotes a vector concatenation. A limitation of this parametrization is that the behaviour will be very suboptimal when ω is not close to 0 or π (Pollard, 2000).

2.3 Averaging Method

The variational dynamics of the MEE are inherently stiff, since the orbital elements vary slowly while the anomaly L varies quickly. Averaging methods allow us to eliminate L by considering the dynamics used in (Kluever and Conway, 2010):

$$\dot{z}(t) = \frac{1}{T}\int_0^{2\pi} F(z(t), E)\frac{dt}{dE}dE, \tag{8}$$

where we take $z = (p, f, g, k, h)$ and $F(z(t), E)dt/dE$ the Sundman-transformed MEE variational equations acquired by multiplying (1a)-(1e) with (2) (leaving out the dynamics for L given in (1f)). Note that we need to eliminate the dependency on τ by using the closed-loop control law $Q_\tau(x,p)$ presented in the previous section *i.e. by substituting* (7) *into* (1). The evaluation of the integral in (8) is done through Gaussian quadrature. We find the nodes E_G and weights w_G using the algorithm described in (Trefethen, 2008). Using the thrust structure described by (5) we can spread out the quadrature points over the integration interval by considering the transformed nodes:

$$\bar{E}_G = \left(p_{E_0}E_G,\ p_{E_\pi}E_G + \bar{\omega} + \pi\right),$$

where the brackets again denote a vector concatenation. The associated quadrature weights then become: $\bar{w}_G = (p_{E_0}w_G,\ p_{E_\pi}w_G)$. Note that (1) still depends on L therefore we need to evaluate the L associated with the elements of $\bar{E}_G$ by inverting (6).

2.4 Sequential Approach

To formulate the optimal control problem, based on the dynamics described in the previous section we will employ the sequential approach (Rawlings et al., 2017). This involves solving the following optimization problem:

$$\begin{aligned} \underset{u}{\textbf{min}} \quad & \ell(u) = \sum_{k=0}^{K} \ell_k(u_k, \psi_k(u)) \\ \textbf{s.t.} \quad & u_k \in \mathcal{U}, \quad \forall k = 0 \dots K-1 \\ & x_0 = \bar{x}, \quad \psi_K(u) = z_f, \end{aligned} \tag{9}$$

where $u_k = (p_{1,k}, p_{2,k}, p_{3,k}, p_{4,k}, p_{E_0,k}, p_{E_\pi,k}, \bar{\omega}_k, p_{rt}, p_n) \in \mathbb{R}^{n_u}$ denotes the discretized inputs, $u = (u_0, \dots, u_{K-1}) \in \mathbb{R}^{n_u K}$ and $\mathcal{U} \subset \mathbb{R}^{n_u}$ denotes the set of feasible inputs, given by $p_{E_0} \geq 0$, $p_{E_\pi} \geq 0$, $p_{E_0} + p_{E_\pi} \leq \pi$ and $p_{rt}^2 + p_n^2 = 1$. $x_0 = (p_0, f_0, g_0, k_0, h_0, L_0) \in \mathbb{R}^{n_x}$ denotes the initial state vector and $z_f \in \mathbb{R}^{n_x - 1}$ denotes the target orbital elements $(p_f, f_f, g_f, k_f, h_f)$, where the constraint on L is omitted since only the shape of the final orbit matters. The dynamics are enforced by using $\psi_k(u) : \mathbb{R}^{n_u K} \to \mathbb{R}^{n_x - 1}$, which corresponds to the numerical integration of the averaged dynamics from t_0 to $t_0 + kT_s$, with $T_s = t_f/K$ the sample time, K the amount of integration intervals and t_f the time of the transfer. We use a RK4 integrator for the numerical integration, where the input is applied using zero-order hold.

For the continuous-time case the cost of the optimization problem is given by $\ell(u) = \int_{t_0}^{t_f} Q_\tau(x(t), p(t))\,\mathrm{d}t$, which is related to the Δv and indirectly to the fuel usage. As such we can introduce an extra state $\dot{x}_\ell(t) = Q_\tau(x(t), p(t))$ that keeps track of the used Δv. Since this state follows dynamics just like all of the other states, averaging can be applied on these as well. The stage cost $\ell_k(u_k, x_k)$ then corresponds to the increment in x_ℓ over time step k as evaluated by the RK4 integrator.

3. FAST NUMERICAL OPTIMIZER

This section presents the proximal averaged Newton-type method for optimal control (PANOC), which is described in (Stella et al., 2017). It is a structured optimization

algorithm ideal for operation on systems with little available memory/performance. The iterative algorithm takes steps that are a weighted average between steps provided by forward-backward stepping (FBS) and quasi-Newton methods. As such it gains the advantages from both methods; the fast convergence of the quasi-Newton methods and the global convergence of FBS, which is maintained by using the forward-backward envelope (FBE) as a merit function for determining the weighting in the average. The algorithm solves problems of type:

$$\min_{u\in\mathcal{U}} \varphi(u), \tag{10}$$

where the cost $\varphi(u)$ is continuously differentiable in u with a Lipschitz-continuous gradient and where $\mathcal{U}$ is a possibly nonconvex set onto which it is easy to project. In our case the differentiability does not hold globally, however this does not cause issues since, in practice, the optimization variables remain in the differentiable region while optimizing. Also note that the input constraint $\mathcal{U} = \mathcal{U}_1 \times \mathcal{U}_2 \times \mathcal{U}_3 \times \mathcal{U}_4$ is seperable. Therefore the projection on $\mathcal{U}$ can be defined as a concatenation of Euclidean projections onto the components $\mathcal{U}_{1,\dots,4}$. The projection for $\mathcal{U}_1 = \mathbb{R}^4$ is the identity map given by: $P_{\mathcal{U}_1}(p_1,p_2,p_3,p_4) = (p_1,p_2,p_3,p_4)$. For the projection onto $\mathcal{U}_2 = \left\{(p_{E_0},p_{E_\pi}) \in \mathbb{R}^2 \middle| p_{E_0} \geq 0, p_{E_\pi} \geq 0, p_{E_0} + p_{E_\pi} \leq \pi\right\}$ associated with the thrust parametrization inputs we get the following:

$$\begin{aligned} P_{\mathcal{U}_2}(p_{E_0,k}, p_{E_\pi,k}) = (& \\ &\left(\tfrac{1}{2}\right) \max\left\{0, \min\left[2\pi, p_{E_0,k} + \min(p_{E_0,k}, \pi - p_{E_\pi,k})\right]\right\}, \\ &\left(\tfrac{1}{2}\right) \max\left\{0, \min\left[2\pi, p_{E_\pi,k} + \min(p_{E_\pi,k}, \pi - p_{E_0,k})\right]\right\}), \end{aligned}$$

which is a simplification of the projection onto a general intersection between a half-space and a box derived in (Beck, 2017, Chapter 6). The projection onto $\mathcal{U}_3 = \mathbb{R}$ is again the identity map: $P_{\mathcal{U}_3}(\bar{\omega}) = \bar{\omega}$. And the projection onto $\mathcal{U}_4 = \left\{(p_{rt},p_n) \in \mathbb{R}^2 \middle| p_{rt}^2 + p_n^2 = 1\right\}$ is given by:

$$P_{\mathcal{U}_{8,9}}(p_{rt},p_n) = \frac{(p_{rt},p_n)}{\sqrt{p_{rt}^2 + p_n^2}}.$$

Given these mappings, the problem described in (10) is compatible with (9). The constraint $\psi_K(u) = z_f$ is the only exception, since it is intractable to evaluate the associated projection. Hence we instead enforce the constraint by adding an extra term to the cost function that penelizes deviations from z_f. The augmented Lagrangian method (Bertsekas, 1996) does this by including both a quadratic term $\mu\|\psi_K(u) - z_f\|^2/2$ and a term containing an estimate of the Lagrangian multipliers $\langle \psi_K(u) - z_f, \lambda\rangle$. The algorithm then works by starting from an initial guess of the multipliers λ_k and solving (10) for an ϵ-approximate stationary point u^* by using PANOC, where $\varphi(u)$ in (10) contains both the cost function $\ell(u)$ and the penalty terms. The estimate is then updated according to $\lambda_{k+1} = \lambda_k - \mu(\psi_K(u^*) - z_f)$. If the residual $w_k = \mu^{-1}\|\lambda_{k+1} - \lambda_k\|$ is smaller then a tolerance δ then the algorithm returns a solution. If the residual is decreased sufficiently, *i.e.* w_{k+1}/w_k *smaller than a parameter* ϑ, then the penalty parameter μ and tolerance ϵ remain the same. Otherwise μ is multiplied by $\varrho > 1$ and the tolerance is divided by $\beta > 1$. A version of this algorithm with only the quadratic penalty was implemented in (Hermans et al., 2018) and compared to other state-of-the-art optimization algorithms.

4. NUMERICAL RESULTS

In this section the heuristic approach developed in Section 2 is applied to a realistic transfer scenario presented in (Koppel, 1999). The result is compared to that of the sequential approach applied to the unregularized dynamics. To correct the integration error due to averaging a closed-loop controller scheme is also presented and validated.

4.1 Comparison with classical sequential approach

The heuristic approach is validated by comparing it to the classical sequential approach, where we integrate over the Sundman-transformed MEE variational dynamics instead of the averaged dynamics. It is used as a reference since the resulting optimization problem can be solved using PANOC. As mentioned before, integrating the Sundman-transformed dynamics corresponds to integrating over the eccentric anomaly E instead of over time. Another terminal state constraint $t(E_f) \leq t_f$ is therefore introduced, where E_f is the eccentric anomaly at the end of the transfer and time $t(E)$ is added as an additional state. To add some flexibity to the solution, E_f is introduced as a variable in the optimization problem. The variables are then the elements of the thrust vector τ in each discretized interval and E_f. The terminal state constraints are once again enforced using ALM.

We consider the transfer described in (Koppel, 1999) starting from an orbit with $a = 36\,463.5$km, $e = 0.818$, $\Omega = \omega = 0°$ and inclination $i = 28.5°$. The target orbit is a geostationary orbit with $a = 42\,157$km and $e = i = 0$. We consider a satellite with $\tau_m = 3 \cdot 10^{-4}$m/s. The optimizer is tuned with $\delta = 10^{-3}$, $\mu_0 = 60$, $\varrho = 2$, $\epsilon_0 = 0.1$, $\beta = 1.2$ and $\vartheta = 0.95$ for both approaches. The evaluation of the gradient of $\varphi(u)$, which is required by PANOC, is done by using CasADi (Andersson et al., 2016), an algorithmic differentiation toolbox. For the sequential approach we add a constraint $E_f < 200 \cdot 2\pi$ and take $t_f = 250$ days. The duration of the sequential transfer is provided to the heuristic approach as the transfer time in order to create a comparable transfer setup. For the sequential approach we needed 12 000 integration steps before finding a good solution, while the heuristic approach worked with only 150 integration intervals. The fact that we can reduce the amount of intervals explains the massive performance boost associated with the heuristic approach. To evaluate the integral in (8) we used 30 quadrature nodes in total.

The results for both the heuristic and the sequential approach are depicted in Figure 2, where the optimal Δv is 1.7891km/s and 1.7535km/s for the heuristic approach and the sequential approach respectively (note that the theoretical optimum is $\Delta v = 1.6676$km/s, which is achieved for impulsive trajectories). The difference is explained by the fact that the control laws reduce the degrees of freedom in the heuristic optimization problem. The total transfer length is 217.43 days. The heuristic transfer is visualised in Cartesian coordinates in Figure 3, where the red curves depict the arcs where thrust is applied. The optimization process took 16 iterations of ALM and a total of 755 inner iterations of PANOC for a CPU time of 9.23 minutes which is a massive improvement compared to the 59.2 minutes required by the sequential approach when applied to the

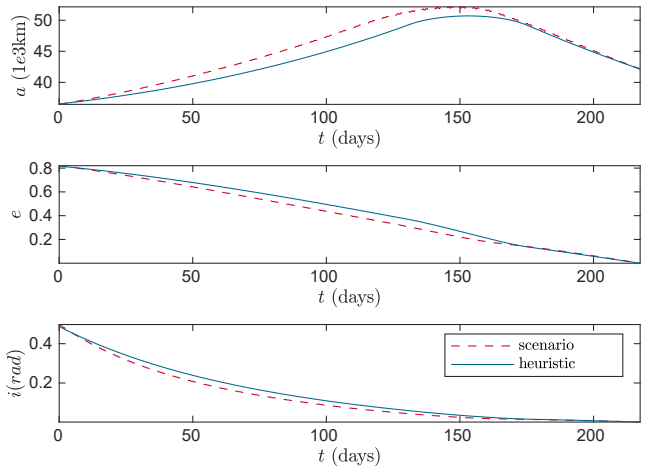


Fig. 2. The state trajectory for the long transfer with inclination change and a relaxed revolution constraint, acquired using the heuristic and sequential approach.

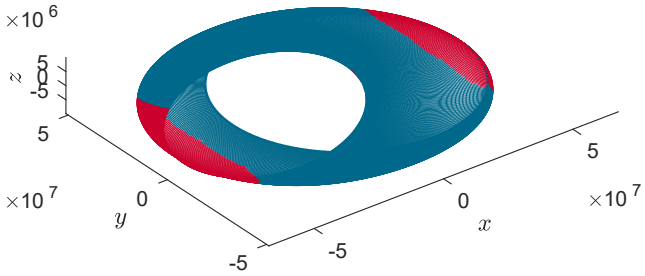


Fig. 3. The trajectory for the long transfer with inclination change acquired using the heuristic method. The coordinate system is earth-centric (Macdonald, 2014).

same problem [3]. Approximately 70% of that time was spend on evaluating the gradient, showing that it is the main bottleneck in the design.

Note that due to the integration error associated with the averaging method, the terminal orbit deviates 1035 km in a, 0.0385 in e and 0.0124° in i from the target orbit. To compensate for this error, the heuristic approach can be applied in a Model Predictive Control (MPC) scheme (Rawlings et al., 2017) described in the next section. The sequential approach would require less compensation.

4.2 Closed-Loop Heuristic Approach

To correct the integration error identified in the previous section we design a scheme that corrects the integration error online. The setup consists of the optimizer described in the previous section, which provides a sequence of inputs u_k. The first input u_0 is then applied for $T_s = t_f/K$ seconds and the evolution of the state is evaluated by a RK4 integrator applied to the MEE variational dynamics. The new value of the state is then assigned to $\bar{x}$ in (9) and the optimization problem is solved once more, but now for a horizon with $K-1$ integration intervals. This process is repeated until the target destination is reached. Note that the additional cost associated with the repeated solution

[3] Tested on a Dell XPS 13 - 9360 developer edition, running Ubuntu 16.04 (Intel i7 quadcore, 16GB of RAM).

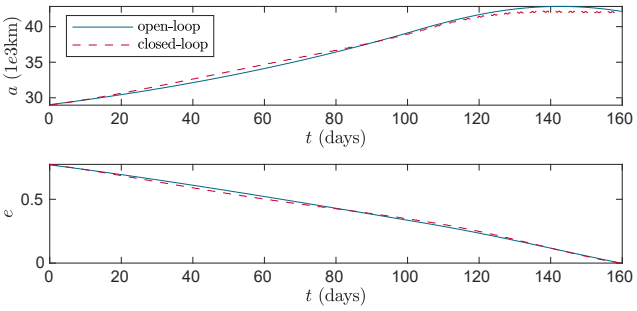


Fig. 4. The state trajectory for the open-loop and closed-loop transfers for a many-revolution transfer.

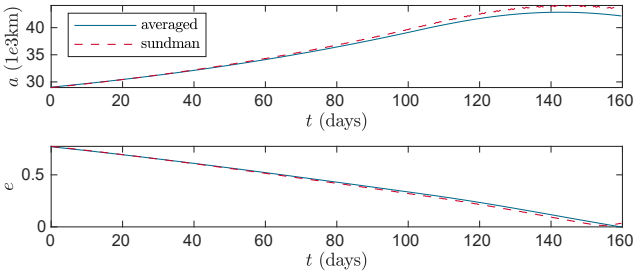


Fig. 5. The state trajectory for the long transfer acquired using the heuristic method. Both the Sundman-transformed and averaged dynamics are depicted.

of (9) is limited since the solution from the previous iteration [4] can be used as an initial guess.

The setup is validated by applying it to a simplified version of the problem described in the previous section where we consider the inclination of the initial orbit to be zero. The parameters of the optimization algorithm are kept the same. The optimal trajectory for the open-loop solution and the closed-loop trajectory are compared in Figure 4. Note that the open-loop trajectory is not exact since it is integrated using the averaged dynamics, while the closed-loop trajectory is more accurate. The required Δv for the closed-loop trajectory is 1.5656km/s, which is less then the open-loop Δv of 1.6107km/s. In fact the cost becomes comparable with the solution found by the sequential approach (1.56km/s) and the theoretical optimum (1.47km/s). Figure 5 illustrates the reason by depicting the open-loop trajectory when integrated through the Sundman-transformed dynamics and the averaged dynamics. Note that the satellite overshoots the target orbit. As such the closed-loop scheme is able to detect this overshoot and corrects it by applying less thrust, especially by the end of the transfer. This behaviour is depicted in Figure 6, which shows the thrust control-law parameters over time. Such fuel-saving would not occur if the error due to averaging would be corrected by using a reference tracker that attempts to track the open-loop trajectory.

5. CONCLUSION

A heuristic approach based on control laws and averaging was derived and applied to a realistic transfer scenario. The averaging of the dynamics introduces an integration error, which is corrected using a closed-loop control

[4] Both u^* and λ^* are passed to the next iteration as well as the final value of μ and ϵ.

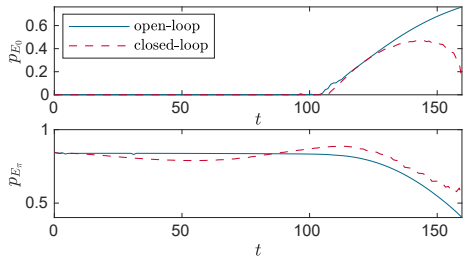


Fig. 6. The fuel related inputs for the open-loop and closed-loop transfers for a many-revolution transfer.

scheme. The resulting performance closely approximates that of the sequential approach, showing that the suboptimality expected from the heuristic approach is minimal. Further improvements are possible by dropping the constant mass assumption, which would make the dynamics more accurate. Other control-laws and better gradient evaluation, *i.e. the algorithmic differentiation executed by CasADi*, could significantly reduce computation time.

REFERENCES

Andersson, J., Gillis, J., and Diehl, M. (2016). User Documentation for CasADi v3.1.0.

Battin, R.H. (1999). *An introduction to the mathematics and methods of astrodynamics, Revised Edition*. AIAA.

Beck, A. (2017). *First-Order Methods in Optimization*. SIAM.

Bertsekas, D.P. (1996). *Constrained optimization and Lagrange multiplier methods*. Athena Scientific.

Betts, J.T. and Erb, S. (2003). Optimal low-thrust trajectories to the moon. *SIAM Jounal Applied on Dynamical Systems*, 2(2), 144–170.

Bruno, C. (2014). Spacecraft Propulsion. In *The International Handbook of Space Technology*, 279–321. Springer-Verlag.

Chachuat, B. (2007). Nonlinear and Dynamic Optimization: From Theory to Practice. Switzerland: Automatic Control Laboratory, EPFL.

Conway, B.A. (2010). *Spacecraft Trajectory Optimization*. Cambridge University Press.

Edelbaum, T.N. (1965). Optimum power-limited orbit transfer in strong gravity fields. *AIAA Journal*, 3(5), 921–925.

Fernandes, S.S. and Carvalho, F.d.C. (2018). Analytical Solution for Optimal Low-Thrust Limited-Power Transfers Between Non-Coplanar Coaxial Orbits. *Journal of Aerospace Technology and Management*, 10(1).

Feuerborn, S.A., Perkins, J., and Neary, D.A. (2013). Finding a Way: Boeing's All Electric Propulsion Satellite. In *Proceedings of the 49th Joint Propulsion Conference*, volume 7, 5615–5619.

Hermans, B., Patrinos, P., and Pipeleers, G. (2018). A penalty method based approach for autonomous navigation using nonlinear model predictive control. In *Proceedings of 6th IFAC Conference on NMPC*, 234 – 240.

Hintz, G.R. (2008). Survey of Orbit Element Sets. *Journal of Guidance, Control, and Dynamics*, 31(3), 785–790.

Huang, R., Hwang, I., and Corless, M. (2009). A new nonlinear model predictive control algorithm using differential transformation with application to interplanetary low-thrust trajectory tracking. In *Proceedings of the 27th American control Conference*, 4868–4873.

Kluever, C.A. (1998). Simple Guidance Scheme for Low-Thrust Orbit Transfers. *Journal of Guidance, Control, and Dynamics*, 21(6), 1015–1017.

Kluever, C.A. and Conway, B. (2010). Low-thrust trajectory optimization using orbital averaging and control parameterization. In *Spacecraft Trajectory Optimization*, 112–138. Cambridge Univiversity Press.

Koppel, C.R. (1999). Advantages of a Continuous Thrust Strategy from a Geosynchronous Transfer Orbit, Using High Specific Impulse Thrusters. In *Proceedings of the 14th International Symposium on Space Flight Dynamics*, 8–12.

Lev, D.R., Emsellem, G.D., and Hallock, A.K. (2017). The Rise of the Electric Age for Satellite Propulsion. *New Space*, 5(1), 4–14.

Macdonald, M. (2014). Introduction to Astrodynamics. In *The International Handbook of Space Technology*, 61–98. Springer-Verlag.

Mazzini, L. (2014). Finite thrust orbital transfers. *Acta Astronautica*, 100(1), 107–128.

Petropoulos, A.E. (2005). Refinements to the Q-law for low-thrust orbit transfers. In *Proceedings of the 15th Space Flight Mechanics Conference*, volume 120, 963–982.

Petropoulos, A.E. and Longuski, J.M. (2004). Shape-Based Algorithm for the Automated Design of Low-Thrust, Gravity Assist Trajectories. *Journal of Spacecraft and Rockets*, 41(5), 787–796.

Pollard, J.E. (2000). Simplified Analysis of Low-Thrust Orbital Maneuvers. Technical Report TR-2000 (8565)-10, Aerospace Corporation.

Prussing, J.E. (2010). Primer vector theory and applications. In *Spacecraft Trajectory Optimization*, 16–36. Cambridge University Press.

Rawlings, J.B., Mayne, D.Q., and Diehl, M.M. (2017). *Model predictive control: theory, computation, and design*. Nob Hill Publishing, 2nd edition.

Schäff, S. (2016). Low-thrust multi-revolution orbit transfers. In *Space Engineering: Modeling and Optimization with Case Studies*, 337–367. Springer International Publishing.

Stella, L., Themelis, A., Sopasakis, P., and Patrinos, P. (2017). A simple and efficient algorithm for nonlinear model predictive control. In *Proceedings of the 56th Annual Conference on Decision and Control*, 1939–1944.

Trefethen, L.N. (2008). Is gauss quadrature better than clenshaw–curtis? *SIAM review*, 50(1), 67–87.

Vicens, J.R. (2016). *Regularization in Astrodynamics: applications to relative motion, low-thrust missions, and orbit propagation*. Ph.D. thesis, Universidad Politécnica de Madrid.

Walker, M., Ireland, B., and Owens, J. (1985). A set modified equinoctial orbit elements. *Celestial Mechanics*, 36(4), 409–419.